

Non-Gaussianity in Multi-field Stochastic Inflation with the Scaling Approximation

Takeshi Hattori and Kazuhiro Yamamoto

Graduate School of Sciences, Hiroshima University, Higashi-hiroshima, 739-8526, Japan

Abstract. The statistics of multi-field inflation are investigated using the stochastic approach. We analytically obtain the probability distribution function of fields with the scaling approximation by extending the previous work by Amendola. The non-Gaussian nature of the probability distribution function is investigated decomposing the fields into the adiabatic and isocurvature components. We find that the non-Gaussianity of the isocurvature component can be large compared with that of the adiabatic component. The adiabatic and isocurvature components may be correlated at nonlinear order in the skewness and kurtosis even if uncorrelated at linear level.

1. Introduction

The inflationary universe is now the standard paradigm that explains the observed universe naturally [1, 2]. One of the most important predictions of inflation is the primordial fluctuations from which the large scale structure of the universe originates. Many models of the inflation have been proposed. Multi-field inflation is a natural alternative model to the standard single field inflaton model (e.g., [3, 4, 5, 6, 7]). In such the multi-field inflation model, the isocurvature perturbation arises in addition to the adiabatic one, though the evolution of the isocurvature perturbations is model-dependent. Testing predictions of these inflation models will be the subject of the (future) precision cosmology by confronting with observation. Statistics of the primordial fluctuations is very important in such the test of the inflation models. In particular, the non-Gaussian nature of the primordial fluctuations is considered to be an important clue [8], which stimulates the recent investigations on the higher order cosmological perturbations [9, 10, 11, 12, 13, 14, 15, 16, 17, 18, 19, 20].

The stochastic inflation was developed by Starobinsky and many works have been done [21, 22, 23, 24]. The stochastic approach to inflation is useful in investigating the statistics of the fluctuations [25, 26]. In the stochastic inflation, the field dynamics coarse-grained over the horizon size is described by the Langevin equation, and the field value of the inflaton is the probability variable. Instead of solving the Langevin equation, we may solve the corresponding Fokker-Planck equation, which describes the evolution of the probability function $P(\phi)$. It is known that the scaling approximation

is useful to describe the evolution of the probability function during the slow-roll period [27]. With the use of the scaling approximation, the probability function can be obtained analytically [28]. The stochastic approach to the multi-field inflation has been considered in [29, 30, 31]. The probability function for the multi-field inflation was constructed using the scaling approximation in an analytic manner by Amendola [31]. However, the constructed probability function does not have the symmetry in exchanging the field parameters. Such the symmetry is desired for a consistency of the theory. As an extension of this previous work, we develop a useful analytic formula for the probability function of the multi-field stochastic inflation using the scaling approximation.

The organization of the present paper is as follows: In section 2, we summarize the stochastic approach to the multi-field inflation. Then we obtain the probability distribution function using the scaling approximation as an extension of the work by Amendola [31]. In section 3, based on the probability function, we investigate the non-Gaussian feature of the scalar fields during the inflation by decomposing the scalar fields into the adiabatic and the isocurvature components. In section 4, we mention about connecting our result with observation. Section 5 is devoted to summary and conclusions. Throughout this paper we use the unit $c = \hbar = 1$, and follow the convention $(+, -, -, -)$.

2. Formulation

We consider the chaotic inflation model with the two scalar fields ϕ and χ with the Lagrangian density

$$\mathcal{L} = \frac{1}{2}\nabla^\mu\phi\nabla_\mu\phi - V_1(\phi) + \frac{1}{2}\nabla^\mu\chi\nabla_\mu\chi - V_2(\chi), \quad (1)$$

where $V_1(\phi)$ and $V_2(\chi)$ are the potential,

$$V_1(\phi) = \frac{\lambda_1}{2n}\sigma^4\left(\frac{\phi}{\sigma}\right)^{2n}, \quad (2)$$

$$V_2(\chi) = \frac{\lambda_2}{2n}\sigma^4\left(\frac{\chi}{\sigma}\right)^{2n}. \quad (3)$$

where λ_1 and λ_2 are the non-dimensional coupling constants, n is the parameter, and we introduced $\sigma^{-2} = 8\pi G$. During the slow-roll regime, neglecting the kinetic terms, the Friedman equation gives

$$H^2 = \frac{V_1(\phi) + V_2(\chi)}{3\sigma^2}, \quad (4)$$

where $H = \dot{a}(t)/a(t)$ is the Hubble parameters, $a(t)$ is the scale factor, the dot denotes the derivative with respect to the cosmic time t .

We adopt the stochastic approach to the inflation. The basic equation, the Langevin equation, is obtained by coarse-graining the field, averaging over the short wave length modes of the evolution equation of the field operator. For the two-field inflation, we have

$$\dot{\phi} = \frac{-V_{1,\phi}}{3H} + g\eta_\phi \quad (5)$$

$$\dot{\chi} = \frac{-V_{2,\chi}}{3H} + g\eta_\chi, \quad (6)$$

where

$$g = \frac{H^{3/2}}{\sigma^{1/2}}, \quad (7)$$

and η_ϕ and η_χ describes the stochastic noises, which have the nature of the Morkovian Gaussian noise with zero mean and the correlation

$$\langle \eta_i(t) \rangle = 0, \quad (8)$$

$$\langle \eta_i(t)\eta_j(t') \rangle = \delta_{ij} \frac{\sigma}{4\pi^2} \delta(t-t'), \quad (9)$$

where η_i and η_j denote η_ϕ and η_χ . Thus the long-range scalar fields during the slow-roll regime are described by the Langevin equations with the classical drift force $-V_{1,\phi}/3H$ or $-V_{2,\chi}/3H$ and the noise whose amplitude is in proportion to g . Note that, even if the field potentials consist of independent function of ϕ and χ , the dynamics is coupled to each other because the Hubble parameter H depends on the both fields. Note that we have assumed $\langle \eta_\phi(t)\eta_\chi(t') \rangle = 0$, based on the assumption that the fine-grained component of the field ϕ and χ can be treated as free in the leading approximation [29, 31]. Then, we may assume the Langevin equations for these field with the Gaussian noise with the correlation $\langle \eta_\phi(t)\eta_\phi(t') \rangle = \langle \eta_\chi(t)\eta_\chi(t') \rangle \propto \delta(t-t')$, in a similar way to the single field stochastic inflation. However, this assumption might be oversimplified for the models with general coupling between ϕ and χ .

Here let us consider the background solution for the Langevin equation without the noise term,

$$\dot{\phi}_{cl} = \frac{-V_{1,\phi}}{3H}, \quad (10)$$

$$\dot{\chi}_{cl} = \frac{-V_{2,\chi}}{3H}. \quad (11)$$

From these zero-noise field equations, we have

$$\frac{d\phi_{cl}}{d\chi_{cl}} = \frac{\lambda_1 \phi_{cl}^{2n-1}}{\lambda_2 \chi_{cl}^{2n-1}}, \quad (12)$$

which gives the attractor solution, assuming that the classical paths converge to it after a short transient,

$$\phi_{cl} = L^{1/2(n-1)} \chi_{cl}, \quad (13)$$

where $L = \lambda_2/\lambda_1$. In the present paper, we refer to the attractor solution as the classical solution. We will solve the Fokker-Planck equation corresponding to the Langevin equation, along the classical attractor trajectory. For the latter convenience, we introduce the parameter θ by

$$\cos \theta = \frac{\dot{\phi}_{cl}}{\sqrt{\dot{\phi}_{cl}^2 + \dot{\chi}_{cl}^2}} = (1 + L^{1/(1-n)})^{-1/2} \quad (14)$$

$$\sin \theta = \frac{\dot{\chi}_{cl}}{\sqrt{\dot{\phi}_{cl}^2 + \dot{\chi}_{cl}^2}} = (L^{1/(n-1)} + 1)^{-1/2}. \quad (15)$$

Our formulation relies on rewriting the Langevin equation in term of the variables r and Θ , introduced in the below, instead of ϕ and χ . First, we define the variable r by

$$r = \phi \cos \theta + \chi \sin \theta. \quad (16)$$

From the Langevin equation for ϕ and χ , we may write

$$\dot{r} = \frac{-\tilde{\lambda}\sigma^3}{3H} \left(\frac{r}{\sigma}\right)^{2n-1} + g(\cos \theta \eta_\phi + \sin \theta \eta_\chi), \quad (17)$$

where H should be regarded as

$$H^2 = \frac{1}{3\sigma^2} (V_1(r \cos \theta) + V_2(r \sin \theta)) = \frac{\tilde{\lambda}\sigma^2}{6n} \left(\frac{r}{\sigma}\right)^{2n} \quad (18)$$

with defined

$$\tilde{\lambda} = \lambda_1 \cos^{2n} \theta + \lambda_2 \sin^{2n} \theta = (\lambda_1^{1/(1-n)} + \lambda_2^{1/(1-n)})^{1-n}. \quad (19)$$

The approximation of equation (18) is similar to that in [31]. In the strict sense, H is the function of ϕ and χ , but, in equation (18), H is approximated as $H(\phi, \chi) = H(\phi_{cl}(r), \chi_{cl}(r))$. The other variable Θ is defined as

$$\Theta = \frac{-1}{2(n-1)} \left[\frac{1}{\lambda_1} \left(\frac{\phi}{\sigma}\right)^{2(1-n)} - \frac{1}{\lambda_2} \left(\frac{\chi}{\sigma}\right)^{2(1-n)} \right]. \quad (20)$$

It is easy to show that Θ satisfies

$$\dot{\Theta} = \left(\frac{\eta_\phi}{V_{1,\phi}} - \frac{\eta_\chi}{V_{2,\chi}} \right) g\sigma^2. \quad (21)$$

We consider (17) and (21), instead of the original Langevin equations (5) and (6).

It will be important to mention about the physical meanings of the variable r and Θ . It is clear that r is the variable parallel to the classical trajectory. On the other hand Θ can be regarded to represent the component perpendicular to the classical trajectory. It is worthy to note that the cross correlation of the noise terms in the Langevin equations r and Θ is zero, i.e.,

$$\left\langle (\cos \theta \eta_\phi + \sin \theta \eta_\chi) \left(\frac{\eta_\phi}{V_{1,\phi}} - \frac{\eta_\chi}{V_{2,\chi}} \right) \right\rangle = 0. \quad (22)$$

Now we consider solving the Fokker-Planck equation corresponding to the Langevin equations for r (and Θ). To find the solution analytically, we adopt the scaling approximation, which was done in reference [28] for single inflaton models. In the slow-roll regime of inflation, the drift force dominates the dynamical evolution of the scalar fields, and the quantum noise is small. Then the coarse-grained probability distribution develops a sharp peak around the classical slow-roll solution. This is the basic background that the scaling approximation may be used to describe the behavior of the probability distribution in the slow-roll regime. The Langevin equation for r is similar to that for the single field inflaton model, and we follow the reference [28] to find the analytic solution with the technique of the scaling approximation. In Appendix A,

the derivation of the probability function is described. The analytic probability function can be written as function of ϕ and χ as

$$P_{sc}(\phi, \chi) = \frac{1}{2\pi\sqrt{v_{11}v_{22}}} \exp \left[-\frac{(\xi(\phi, \chi) - \xi_*)^2}{2v_{11}} - \frac{\Theta(\phi, \chi)^2}{2v_{22}} \right] |J(\phi, \chi)|, \quad (23)$$

where $J(\phi, \chi)$ is the Jacobian of the transformation,

$$|J| = |\xi_{,\phi}\Theta_{,\chi} - \xi_{,\chi}\Theta_{,\phi}|, \quad (24)$$

and the variances are obtained as

$$v_{11} = \frac{1}{16\pi^2} \sqrt{\frac{3}{2n\tilde{\lambda}}} \left(\frac{r_*}{\sigma}\right)^{2-n} \left[1 - \left(\frac{r_{cl}}{r_*}\right)^4 \right] \quad (n \geq 2) \quad (25)$$

and

$$v_{22} = \begin{cases} \frac{\tilde{\lambda}}{192\pi^2} \left(\frac{1}{\lambda_1^2 \cos^6 \theta} + \frac{1}{\lambda_2^2 \sin^6 \theta} \right) \left[-\ln \left(\frac{r_{cl}}{r_*} \right) \right] & (n = 2) \\ \frac{\tilde{\lambda}}{96\pi^2 n^2 (n-2)} \left(\frac{1}{\lambda_1^2 \cos^{2(2n-1)} \theta} + \frac{1}{\lambda_2^2 \sin^{2(2n-1)} \theta} \right) & \\ \times \left[\left(\frac{r_{cl}}{\sigma} \right)^{2(2-n)} - \left(\frac{r_*}{\sigma} \right)^{2(2-n)} \right] & (n > 2) \end{cases}, \quad (26)$$

and ξ is related to $r(\phi, \chi)$ by equation (A.6) and $\xi_* = \xi(r_{cl})$.

Here we mention about the boundary condition of the probability distribution function. The reflecting boundary condition, with which the normalization of the probability is preserved, is adopted in usual. In this case, other reflective term should be added to the probability function. However, as long as we are concerning with the behavior of the probability function around the peak of the classical slow-roll solution, we may work with the solution (23) practically.

Figure 1 shows the contours of the probability function to make an example of its time evolution. At the earlier time (left panel), the probability function is almost spherically distributed. At the middle time (center panel), the probability function becomes rather broad, then it becomes elongated along the direction of the classical path at the latter time (right panel). The behavior depends on the model parameters as well as the initial condition.

3. Non-Gaussian behavior of the probability function

In this section we investigate the evolution of the probability function (23), focusing on the non-Gaussian statistical nature. We start from introducing the variable Δr and Δs by

$$\begin{pmatrix} \Delta r \\ \Delta s \end{pmatrix} = \begin{pmatrix} \cos \theta & \sin \theta \\ -\sin \theta & \cos \theta \end{pmatrix} \begin{pmatrix} \phi - \phi_{cl} \\ \chi - \chi_{cl} \end{pmatrix}. \quad (27)$$

We may regard Δr (Δs) as the component that contributes to the adiabatic (isocurvature) perturbation [5, 6]. We rewrite the probability distribution function in

terms of Δr and Δs . The expansion can be done in a straightforward manner. But the expression is rather long, then the result is given in Appendix B.

Here let us introduce the e -folding number from a time t to the final time of the inflation t_f ,

$$N(t) = \int_t^{t_f} H(t') dt', \quad (28)$$

where t_f is defined by $V_1(\phi_{cl}) + V_2(\chi_{cl}) = (\dot{\phi}_{cl}^2 + \dot{\chi}_{cl}^2)/2$, which gives $r_{cl}(t_f)^2 = 2n^2\sigma^2/3$. Instead of using t (or $r_{cl}(t)$), we use N as the time variable. The classical solution is related to N by

$$\left(\frac{r_{cl}(t)}{r_*}\right)^2 = \frac{n+6N}{n+6N_*} \equiv \mathcal{N} \leq 1 \quad (29)$$

for $n \geq 2$, where $N_* = N(t_*)$.

With the use of \mathcal{N} (or N), the part of the probability function of ξ , equation (B.1), is written

$$\begin{aligned} \exp\left[-\frac{(\xi - \xi_*)^2}{2v_{11}}\right] &= \exp\left[-R_n \left\{ \left(\frac{\Delta r}{r_{cl}}\right)^2 \right. \right. \\ &\quad - \left(n-1 + \frac{n+2}{2}\mathcal{N}^{2-n}\right) \left(\frac{\Delta r}{r_{cl}}\right)^3 \\ &\quad + \left(\frac{(n-1)(7n-3)}{12} + \frac{3(n-1)(n+2)}{4}\mathcal{N}^{2-n}\right. \\ &\quad \left. \left. + \frac{(n+2)(30-n)}{48}\mathcal{N}^{2(2-n)}\right) \left(\frac{\Delta r}{r_{cl}}\right)^4 \dots \right\}\right], \quad (30) \end{aligned}$$

and R_n is

$$R_n = \frac{96\pi^2}{\tilde{\lambda}} \left(\frac{3}{2n}\right)^n n^2 (\mathcal{N}^{-2} - 1)^{-1} (n+6N)^{-n} \quad (31)$$

from (B.2). On the other hand, the part of the probability function of Θ is also written in the similar way, i.e., equation (B.3), with

$$S_n = \frac{96\pi^2}{\tilde{\lambda}} \times \begin{cases} \frac{9}{32}(1+3N)^{-2}(-\ln\mathcal{N})^{-1} & (n=2) \\ \frac{(n-2)n^2}{2} \left(\frac{3}{2n}\right)^n (n+6N)^{-n} (1-\mathcal{N}^{n-2})^{-1} & (n>2) \end{cases} \quad (32)$$

From equations (31) and (32) we easily have

$$\frac{S_n}{R_n} = \begin{cases} \frac{1}{2}(\mathcal{N}^{-2} - 1)(-\ln\mathcal{N})^{-1} & (n=2) \\ \frac{n-2}{2}(\mathcal{N}^{-2} - 1)(1-\mathcal{N}^{n-2})^{-1} & (n>2) \end{cases} \quad (33)$$

and $S_n/R_n \geq 1$ (see Figure 2). Because the variance of Δr and Δs is in proportion to $1/R_n$ and $1/S_n$, respectively, then it can be read that the amplitude of the fluctuation of the isocurvature component is smaller than that of the adiabatic component. This is consistent with the behavior of the probability function shown in Figure 1.

We next consider the deviation of the probability function from the Gaussian statistics, which is expressed by the terms in proportion of Δr^3 , Δs^3 , and the other higher order terms. To investigate the deviation of the probability distribution function from the Gaussian statistics quantitatively, we first define the ratio

$$\mathcal{T} \equiv \frac{P_{sc}(+\Delta r, +\Delta s)}{P_{sc}(-\Delta r, -\Delta s)}. \quad (34)$$

Thus \mathcal{T} represents the asymmetry of the probability function, which can be related to the dimensionless skewness (see below). In the limit of the Gaussian statistics, $\mathcal{T} - 1$ approaches to zero. This is a very simple but useful estimator of the local skewness around the Gaussian peak introduced in reference [32]. From our probability function, we have the expression of the leading order

$$\begin{aligned} \mathcal{T} - 1 \approx 2 \left[\left(n - 1 + \frac{n+2}{2} \mathcal{N}^{(2-n)/2} \right) R_n \left(\frac{\Delta r}{r_{cl}} \right)^3 - (2n-1) \Gamma_n S_n \left(\frac{\Delta s}{r_{cl}} \right)^3 \right. \\ \left. + 2(2n-1) S_n \left(\frac{\Delta r}{r_{cl}} \right) \left(\frac{\Delta s}{r_{cl}} \right)^2 \right], \quad (35) \end{aligned}$$

for $n \geq 2$, where Γ_n is defined by (B.5). Our result of the adiabatic component with $n = 2$ reproduces the result in reference [32].

We can read a few characteristic features of the skewness from expression (35). First, the evolution of the skewness, in general, depends on the parameters of the potential. It also depends on the initial time $N(t_*)$, which we have adopted to solve the Fokker-Planck equation. This is unavoidable in our scheme. Let us consider the skewness of the adiabatic component, the first term of the right hand side (r.h.s.) of (35). To estimate the skewness quantitatively, we consider the first term at the one sigma deviation with respect to Δr , with replacing $\Delta r/r_{cl}$ by $1/\sqrt{2R_n}$,

$$A_R = \left(n - 1 + \frac{n+2}{2} \mathcal{N}^{(2-n)/2} \right) \frac{1}{\sqrt{2R_n}}. \quad (36)$$

In the similar way, considering the second term of (r.h.s.) of (35) at the one sigma deviation with respect to Δs , with replacing $\Delta s/r_{cl}$ by $1/\sqrt{2S_n}$, we define

$$A_S = -(2n-1) \Gamma_n \frac{1}{\sqrt{2S_n}}. \quad (37)$$

Figure 3 plots A_R and A_S as function of N for the models $\lambda_1 = \lambda_2 = 10^{-12}$, and $\lambda_1 = 10^{-12}$ and $\lambda_2 = 10^{-13}$. For the model $\lambda_1 = \lambda_2$, we have $A_S = 0$ because $\Gamma_n = 0$. Here we extensively used our result to the case $n = 1.5$. We see that A_S is larger than A_R for the model $\lambda_1 = 10^{-12}$ and $\lambda_2 = 10^{-13}$. Figure 4 plots the same as Figure 3 but with $n = 2$. Similarly, Figures 5 and 6 are same as Figure 3 but with $n = 3$ and $n = 4$, respectively. From Figures 3-6, we see that the non-Gaussian estimator A_R and A_S becomes larger as n becomes larger, in general, depending on $\tilde{\lambda}$. But the ratio of A_S to A_R becomes large as n becomes small. This comes from the fact that the skewness of the isocurvature component A_S is in proportion to Γ_n . Figure 7 plots the ratio A_S/A_R at a fixed time as function of L for various models of n . This result demonstrates that the skewness of the isocurvature component is independent of the adiabatic component,

and can be large compared to the adiabatic one. The asymmetry in the two potentials enhances the non-Gaussianity of the isocurvature component. In reference [33], the importance of the non-Gaussianity of the isocurvature component was discussed in a different context of the investigation of multi-field inflation.

The third term of the r.h.s. of (35) represents the mixing of the isocurvature and the adiabatic components. This suggests that the adiabatic and isocurvature components may have a correlation at nonlinear order in general, even if it have no correlation at the linear order [34].

Similar to the skewness, the terms in proportion to Δr^4 and Δs^4 represent the local kurtosis of the probability function. It can be read that the coefficient of Δs^4 depends on Γ_n but the coefficient of Δr^4 does not. This means that, similar to the case of the skewness, the kurtosis of the isocurvature component is independent of the adiabatic component and can be large compared to it.

4. Connecting the result with observation

Here let us briefly mention about the detectability of the skewness and kurtosis. As mentioned in section 1, many works related to the non-Gaussian nature of the primordial fluctuations have been done. The useful quantity f_{NL} is introduced to characterize the non-Gaussianity of the gravitational potential Φ , by expanding it as [35]

$$\Phi = \varphi + f_{NL}(\varphi^2 - \langle \varphi^2 \rangle) + \mathcal{O}(f_{NL}^2), \quad (38)$$

where φ is a zero-mean Gaussian probability variable. Here assume φ and Φ are the variables with one degree of freedom, it is easy to construct the probability distribution function of Φ ,

$$P(\Phi) \propto \exp \left[-\frac{\Phi^2 - 2f_{NL}\Phi^3}{2\langle \Phi^2 \rangle} \right], \quad (39)$$

neglecting the terms proportional to f_{NL}^2 . ‡ Then we define the local skewness for the probability function $P(\Phi)$, in the similar way to the previous section, by

$$\mathcal{T}_\Phi - 1 = \frac{P(\sqrt{\langle \Phi^2 \rangle})}{P(-\sqrt{\langle \Phi^2 \rangle})} - 1 \simeq 2f_{NL} \langle \Phi^2 \rangle^{1/2}. \quad (40)$$

We can write $\mathcal{T}_\Phi - 1$ in terms of the dimensionless skewness defined by $\langle \Phi^3 \rangle / \langle \Phi^2 \rangle^{3/2}$. Approximating the probability function as

$$\exp \left[-\frac{\Phi^2 - 2f_{NL}\Phi^3}{2\langle \Phi^2 \rangle} \right] \simeq \left(1 + f_{NL} \frac{\Phi^3}{\langle \Phi^2 \rangle} \right) \exp \left[-\frac{\Phi^2}{2\langle \Phi^2 \rangle} \right], \quad (41)$$

we have

$$\frac{\langle \Phi^3 \rangle}{\langle \Phi^2 \rangle^{3/2}} \simeq 15f_{NL} \sqrt{\langle \Phi^2 \rangle} = \frac{15}{2} (\mathcal{T}_\Phi - 1). \quad (42)$$

‡ In deriving this expression we redefined $\Phi + f_{NL} \langle \Phi^2 \rangle$ by Φ to eliminate the term proportional to Φ .

In general, the evolution of fluctuations depends on each model. However, we here introduce the assumption that the dimensionless skewness preserves, that is $|\mathcal{T}_\Phi - 1| \simeq |\mathcal{T} - 1|$, even if the amplitude of the fluctuations may change during the evolution of the universe. Based on this assumption our result can be connected with observation. In this case the predicted local skewness is related to f_{NL} as

$$|\mathcal{T} - 1| = 2f_{NL}\sqrt{\langle\Phi^2\rangle} \quad \text{or} \quad \frac{|\mathcal{T} - 1|}{\sqrt{\langle\Phi^2\rangle}} = 2f_{NL}. \quad (43)$$

If we adopt $\sqrt{\langle\Phi^2\rangle} = 10^{-5}$, the vertical axis of Figures 3-6 can be read as $2f_{NL}$.

The detectable minimum value of f_{NL} is discussed in references [35], $f_{NL} = 20$ and 5 for WMAP and Planck data, respectively. Thus the non-Gaussianity in our model with $n \geq 3$ might be detectable. However, this is based on the rough estimation because we have not strictly considered the observational constraint on the model parameters from the spectrum index and the amplitude of the perturbation. For definite conclusions we need incorporate these constraints.

Similar to the skewness, we can estimate the local kurtosis, being of order $\mathcal{O}(\langle\Phi^2\rangle)$. This is smaller than the skewness by a factor of 10^{-5} .

5. Summary and conclusions

In the present paper, we have investigated the statistical nature of the multi-field inflation with the stochastic approach, in which the evolution of the scalar fields is described by the Langevin equations. To solve the corresponding Fokker-Planck equation analytically, we adopt the technique of the scaling approximation. This was first considered in [31]. We have improved the previous investigation requiring the probability function to have the symmetry in exchanging the field parameters. We have investigated the non-Gaussian nature of the probability function by decomposing the fields into the adiabatic and the isocurvature components.

We have introduced the local skewness as an estimator of the non-Gaussianity, and have found the followings: (1) The amplitude of the skewness is determined by the combination of the coupling constant λ_1 , λ_2 and n . The amplitude of the skewness of the adiabatic component is determined by the combination of the coupling constant $\tilde{\lambda}$ and n , while that of the isocurvature component depends on $\tilde{\lambda}$, n and the ratio of the coupling constant Γ_n . Then the skewness of the isocurvature component can be large compared with that of the adiabatic one due to the factor Γ_n . (2) The similar feature can be seen in the kurtosis of the adiabatic and isocurvature components. (3) The adiabatic and isocurvature components may have correlation at the nonlinear order in the skewness and kurtosis, even if there is no correlation at the linear order.

We have considered the connection between our result and observation, based on the assumption that the dimensionless skewness of fluctuation is preserved. This argument shows that the skewness will be useful to constrain the potential parameter. However the assumption is not trivial and there remains room for more discussions for precise

comparison with observation. Furthermore, in the present paper, we have only worked with the simple chaotic inflation models with the power-low potentials. Investigation of multi-field inflation with more general potentials will be an interesting subject, including the confrontation with cosmic microwave anisotropy observation. Testing the robustness of the approximation adopted here will also be required as a future investigation.

Acknowledgments

This work is supported in part by Grant-in-Aid for Scientific research of Japanese Ministry of Education, Culture, Sports, Science and Technology, No.15740155. We thank B. A Bassett and anonymous referee for useful comments, which helped improve the manuscript. We also thank M. Sasaki for useful conversation related to the topic in the present paper.

References

- [1] Guth A 1981 Phys. Rev. D **23** 374
- [2] Sato K 1981 Mon. Not. R. Astron. Soc. **195** 467
- [3] Mukhanov V F and Steinhardt P J 1998 Phys. Lett. B **422** 52
- [4] Sasaki M and Tanaka T 1998 Prog. Theor. Phys. **99** 763
- [5] Gordon C, Wands D, Bassett B A and Maartens R 2001 Phys. Rev. D **63** 023506
- [6] Amendola L, Gordon C, Wands D and Sasaki M 2002 Phys. Rev. Lett. **88**, 211302
- [7] Parkinson D, Tsujikawa S, Bassett B A and Amendola L 2005, Phys. Rev. D **71**, 063524
- [8] Bartolo N, Komatsu E, Matarrese S and Riotto A 2004 Phys. Rep. **402** 103
- [9] Enqvist K and Vaihkonen A 2004, JCAP 0409, 006
- [10] Vaihkonen A arXiv:(astro-ph/0506304)
- [11] Rigopoulos G I and Shellard E P S, and van Tent B J W arXiv:(astro-ph/0410486)
- [12] Rigopoulos G I and Shellard E P S, arXiv:(astro-ph/0405185)
- [13] Lyth D H, Malik K A and Sasaki M arXiv:(astro-ph/0411220)
- [14] Longlois D and Vernizzi F arXiv:(astro-ph/0503416)
- [15] Lyth D H and Rodriguez Y arXiv:(astro-ph/0502578)
- [16] Lyth D H and Rodriguez Y arXiv:(astro-ph/0504045)
- [17] Boubekeur L and Lyth D H arXiv:(astro-ph/0504046)
- [18] Tomita K 2005 Phys. Rev. D **71** 053504
- [19] Rigopoulos G I, Shellard E P S and van Tent B J W arXiv: (astro-ph/0504508)
- [20] Seery D and Lidsey J E arXiv: (astro-ph/0506056)
- [21] Starobinsky A A 1986 *Field Theory, Quantum Gravity and Strings* ed H J de Vega and N Sanches (Springer Lecture Notes in Physics) 246
- [22] Sasaki M, Nambu Y and Nakao K 1988 Phys. Lett. B **209** 197
- [23] Nakao K, Nambu Y and Sasaki M 1998 Prog. Theor. Phys. **80** 1041
- [24] Sasaki M, Nambu Y and Nakao K 1988 Nucl. Phys. B **308** 868
- [25] Starobinsky A A and Yokoyama J 1994, Phys. Rev. D **50** 6357
- [26] Liguori M, Matarrese S, Musso M and Riotto A 2004, JCAP, 0408, 011
- [27] Suzuki M, 1981 Adv. in Chem. Phys. **46** 195
- [28] Matarrese S, Ortolan A and Lucchin F 1989 Phys. Rev. D **40** 290
- [29] Mollerach S, Matarrese S, Ortolan A and Lucchin F 1991 Phys. Rev. D **44** 1670
- [30] Garcia-Bellido J and Wands D 1995 Phys. Rev. D **52** 5636
- [31] Amendola L 1993 Class. Quantum Grav. **10** 1267
- [32] Yi I, Vishniac E T and Mineshige S 1991, Phys. Rev. D **43**, 362
- [33] Bernardeau F and Uzan J-P 2002, Phys. Rev. D **66** 103506
- [34] Bartolo N, Matarrese S and Riotto A 2001 Phys. Rev. D **64** 083514
- [35] Komatsu E and Spergel D N 2001 Phys. Rev. D **63** 063002

Appendix A. Scaling transformation and probability function

To find the scaling solution of equation (17), two transformation on the variable is performed to yield a Langevin equation with drift term vanished. The first transformation is defined by

$$r \rightarrow z = \int_r^{r_\infty} \frac{dr'}{g(r')}, \quad (\text{A.1})$$

where r_∞ is an arbitrary constant, but we here chose $r_\infty = \infty$ to get z with the same sign of $r (> 0)$. In terms of this new variable, the Langevin equation is

$$\dot{z} = \frac{\tilde{\lambda}\sigma^{7/2}}{3H^{5/2}(r(z))} \left(\frac{r(z)}{\sigma} \right)^{2n-1} - (\cos\theta\eta_\phi + \sin\theta\eta_\chi). \quad (\text{A.2})$$

Thus, with the first transformation, the multiplicative (r -dependent noise) process reduces to the additive (constant noise) process, and the variable z is referred to as the constant-diffusion variable. Then we perform the second mapping, requiring that the resultant Langevin equation has no drift term,

$$z \rightarrow \xi = F^{-1}[e^{\Lambda t}F(z)]. \quad (\text{A.3})$$

The function F is found in the form,

$$F(z) = \exp \left[- \int_{z_*}^z \frac{\Lambda}{D_z} dz' \right], \quad (\text{A.4})$$

where D_z is the drift term of equation (A.2),

$$D_z = \frac{\tilde{\lambda}\sigma^{7/2}}{3H^{5/2}(r(z))} \left(\frac{r(z)}{\sigma} \right)^{2n-1}, \quad (\text{A.5})$$

and $\Lambda = -D_z(z_*)$ is the separation constant and z_* is chosen so that $\partial F(z_*)/\partial z = 1$. Through these transformation, we obtain

$$\xi(r) = \begin{cases} \frac{1}{2} \left(\frac{12}{\tilde{\lambda}} \right)^{3/4} \left(\frac{r}{\sigma} \right)^{-2} \left(\frac{r_{cl}}{r_*} \right)^2 & (n = 2) \\ \frac{2}{3n-2} \left(\frac{6n}{\tilde{\lambda}} \right)^{3/4} & \\ \times \left[\left(\frac{r}{\sigma} \right)^{2-n} - \left(\frac{r_{cl}}{\sigma} \right)^{2-n} + \left(\frac{r_*}{\sigma} \right)^{2-n} \right]^{(3n-2)/(2n-4)} & (n > 2) \end{cases} \quad (\text{A.6})$$

where r_* is the initial value of the classical solution, and we used the classical solution $r_{cl}(t)$, defined as

$$\frac{r_{cl}}{r_*} = \begin{cases} \exp \left[-2\sqrt{\frac{\tilde{\lambda}}{3}}\sigma t \right] & (n = 2) \\ \left[1 + (n-2) \left(\frac{r_*}{\sigma} \right)^{n-2} \sqrt{\frac{2n\tilde{\lambda}}{3}}\sigma t \right]^{1/(2-n)} & (n > 2) \end{cases}, \quad (\text{A.7})$$

which is given by solving equation (17) neglecting the noise term. Now the Langevin equation for ξ is

$$\dot{\xi} = - \left(\frac{\xi}{z} \right)^{(n+2)/(3n-2)} (\cos\theta\eta_\phi + \sin\theta\eta_\chi). \quad (\text{A.8})$$

We follow the standard choice of the initial condition for the probability distribution, the delta-function distribution at the initial time. Furthermore, assuming the limit of small diffusion, we adopt the Gaussian form of the probability distribution function in the scaling approximation

$$P(\xi) \propto \exp \left[-\frac{(\xi - \xi_*)^2}{2v_{11}} \right], \quad (\text{A.9})$$

where v_{11} is given by expression (25), and $\xi_* = \xi(r_{cl})$.

On the other hand the Langevin equation for the variable Θ has no drift term initially, then we write the probability distribution function in the Gaussian form assuming the limit of small diffusion

$$P(\Theta) \propto \exp \left[-\frac{\Theta^2}{2v_{22}} \right], \quad (\text{A.10})$$

where v_{22} is given by (26).

Appendix B. Expansion of the probability function

In this Appendix, we present the expression of the probability function expanded in terms of Δr and Δs . The variable ξ is written in terms of r , equation (A.6). Then the part of the probability function written by ξ provides us with information about the adiabatic component, which can be expanded as follows, by setting $r = r_{cl} + \Delta r$,

$$\begin{aligned} \exp \left[-\frac{(\xi - \xi_*)^2}{2v_{11}} \right] = & \exp \left[-R_n \left\{ \left(\frac{\Delta r}{r_{cl}} \right)^2 \right. \right. \\ & - \left(n - 1 + \frac{n+2}{2} \left(\frac{r_{cl}}{r_*} \right)^{2-n} \right) \left(\frac{\Delta r}{r_{cl}} \right)^3 \\ & + \left(\frac{(n-1)(7n-3)}{12} + \frac{3(n-1)(n+2)}{4} \left(\frac{r_{cl}}{r_*} \right)^{2-n} \right. \\ & \left. \left. + \frac{(n+2)(30-n)}{48} \left(\frac{r_{cl}}{r_*} \right)^{2(2-n)} \right) \left(\frac{\Delta r}{r_{cl}} \right)^4 \dots \right\} \right], \quad (\text{B.1}) \end{aligned}$$

for $n \geq 2$, where we defined

$$R_n = \frac{96\pi^2}{\tilde{\lambda}} n^2 \left[\left(\frac{r_*}{\sigma} \right)^4 - \left(\frac{r_{cl}}{\sigma} \right)^4 \right]^{-1} \left(\frac{r_{cl}}{\sigma} \right)^{2(2-n)}. \quad (\text{B.2})$$

On the other hand, the part of the probability function of Θ is expanded as

$$\begin{aligned} \exp \left[-\frac{\Theta^2}{2v_{22}} \right] = & \exp \left[-S_n \left\{ \left(\frac{\Delta s}{r_{cl}} \right)^2 + (2n-1)\Gamma_n \left(\frac{\Delta s}{r_{cl}} \right)^3 \right. \right. \\ & - 2(2n-1) \left(\frac{\Delta r}{r_{cl}} \right) \left(\frac{\Delta s}{r_{cl}} \right)^2 \\ & + \frac{2n-1}{12} ((14n-3)\Gamma_n^2 + 8n) \left(\frac{\Delta s}{r_{cl}} \right)^4 \\ & \left. \left. - (2n-1)(4n-1)\Gamma_n \left(\frac{\Delta r}{r_{cl}} \right) \left(\frac{\Delta s}{r_{cl}} \right)^3 \right\} \right] \end{aligned}$$

$$+ (2n - 1)(4n - 1) \left(\frac{\Delta r}{r_{cl}} \right)^2 \left(\frac{\Delta s}{r_{cl}} \right)^2 \cdots \left. \right\}, \quad (\text{B.3})$$

where we defined

$$S_n = \frac{96\pi^2}{\tilde{\lambda}} \times \begin{cases} \left[-\ln \left(\frac{r_{cl}}{r_*} \right) \right]^{-1} \left(\frac{r_{cl}}{\sigma} \right)^{4(1-n)} & (n = 2) \\ \frac{(n-2)n^2}{2} \left[\left(\frac{r_{cl}}{\sigma} \right)^{2(2-n)} - \left(\frac{r_*}{\sigma} \right)^{2(2-n)} \right]^{-1} \left(\frac{r_{cl}}{\sigma} \right)^{4(1-n)} & (n > 2) \end{cases} \quad (\text{B.4})$$

and

$$\Gamma_n \equiv \tan \theta - \cot \theta = (1/L)^{1/2(n-1)} - L^{1/2(n-1)}. \quad (\text{B.5})$$

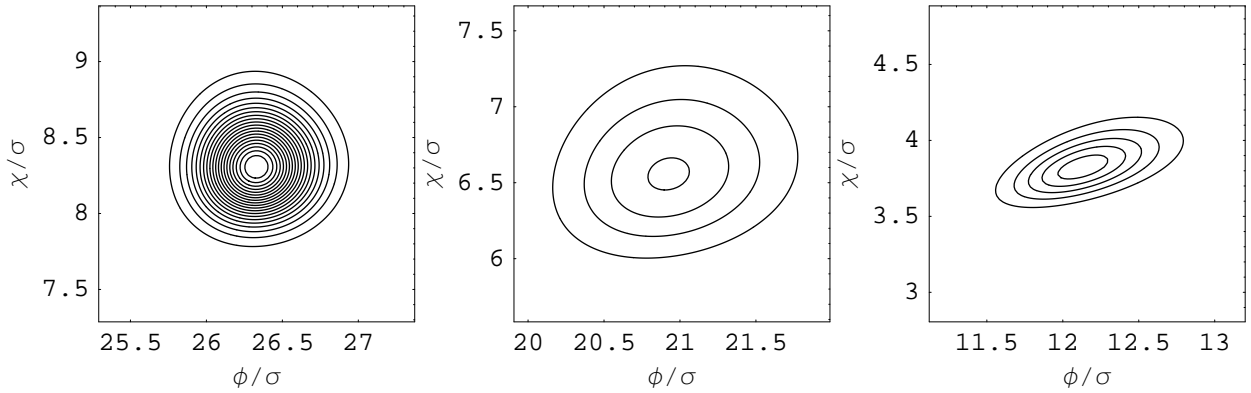


Figure 1. Contours of the probability distribution function. Here the potential with $\lambda_1 = 10^{-5}$, $\lambda_2 = 10^{-4}$, and $n = 2$ is considered. The initial time is chosen $N_* = 100$ and the left, middle and right panels show the contour at the time of the e-folding $N = 95, 60,$ and $20,$ respectively. (See equation (28) for the definition of N)

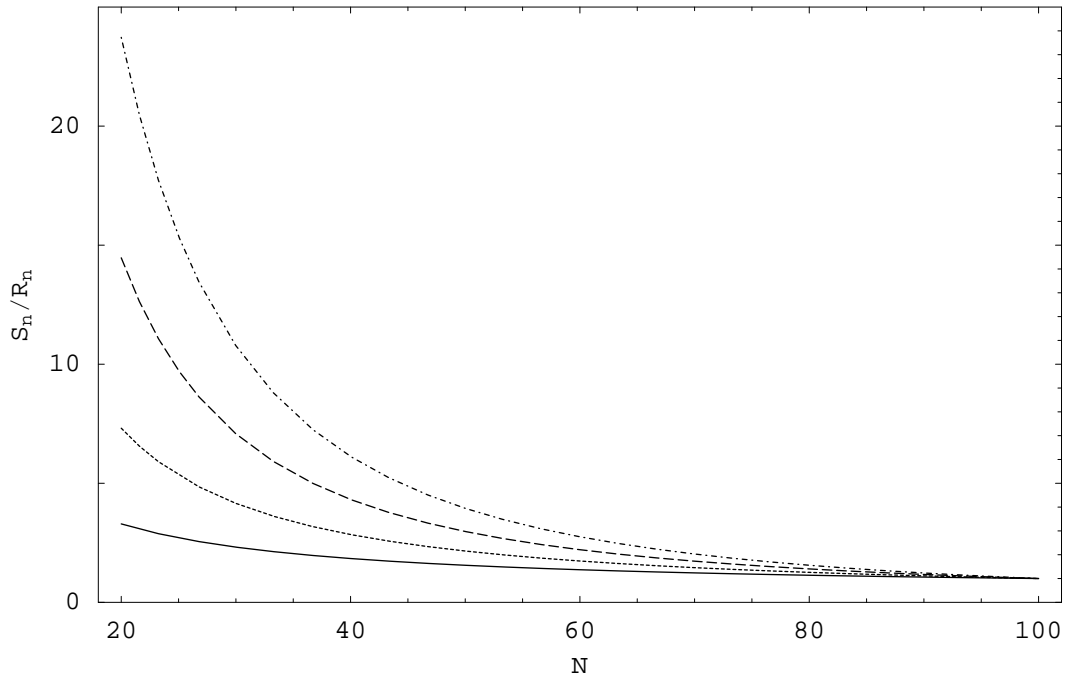


Figure 2. The ratio S_n/R_n is plotted as function of N . The initial time is chosen $N_* = 100$. The parameter of the potential n is chosen $n = 1.1, 2, 3, 4$ from bottom to top. Here we extensively used our result to the case $n < 2$.

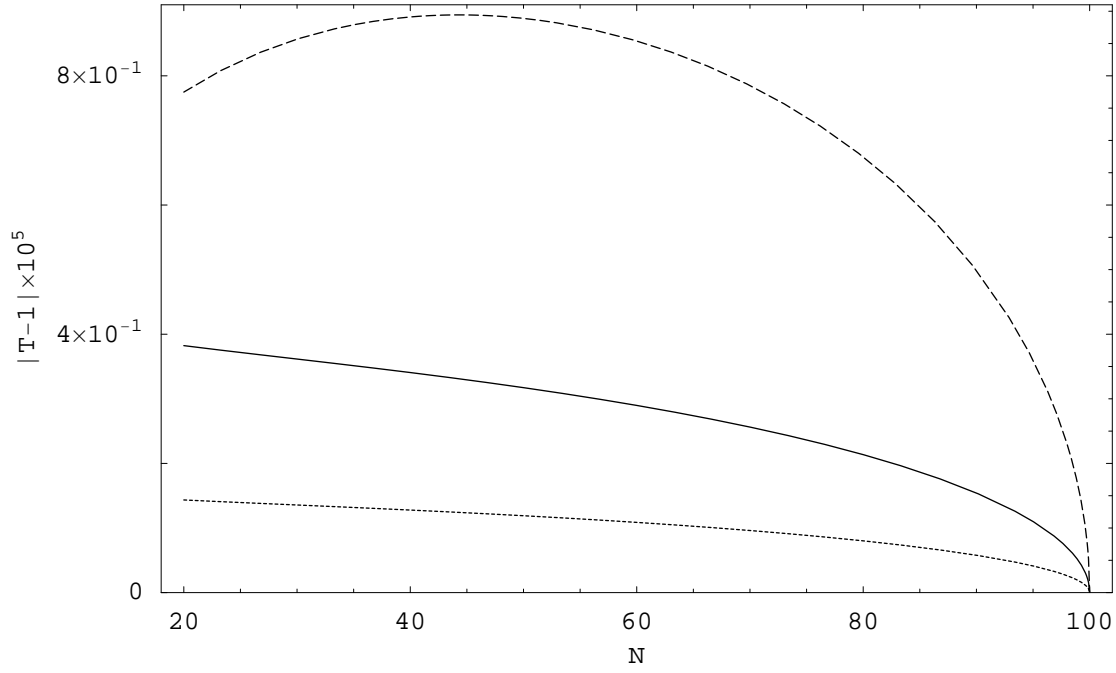


Figure 3. A_R and A_S as function of N . The dotted (dashed) curve plots A_R (A_S) for the model with the parameters $\lambda_1 = 10^{-12}$ and $\lambda_2 = 10^{-13}$, while the solid curve plots A_R with $\lambda_1 = \lambda_2 = 10^{-12}$. Here we adopted $N_* = 100$ and $n = 1.5$.

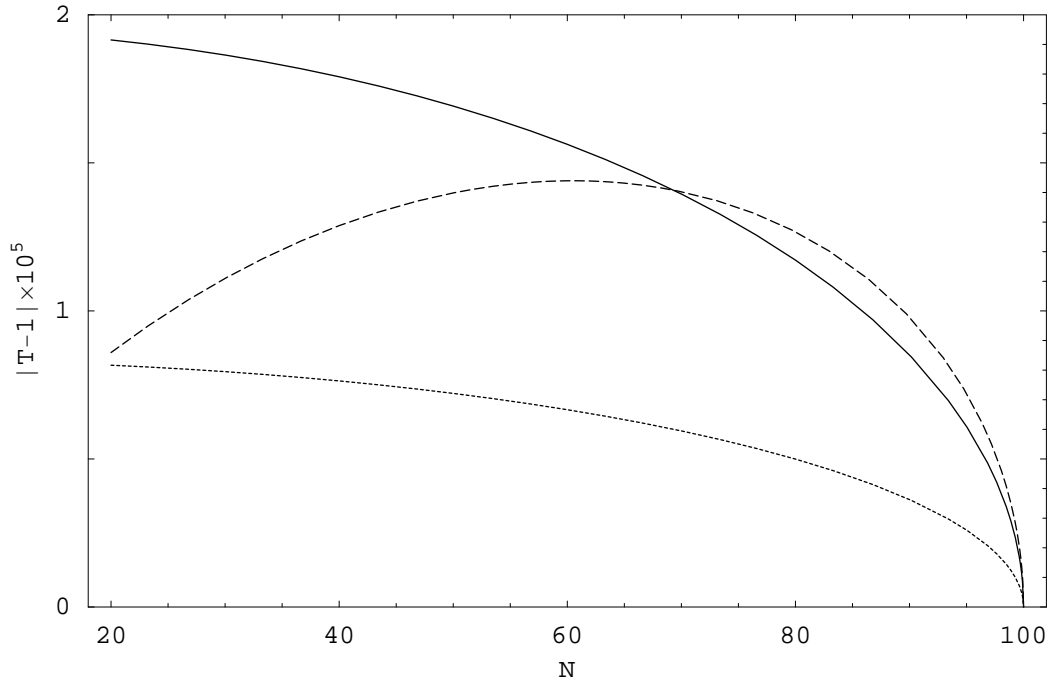


Figure 4. Same as figure 3, but with $n = 2$.

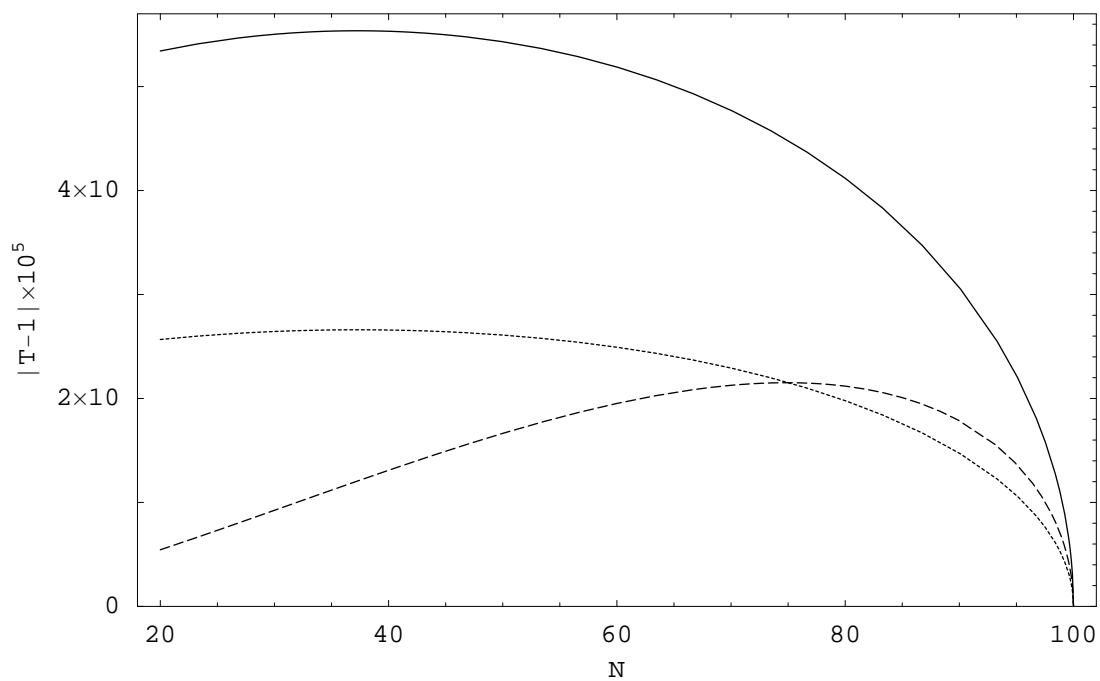


Figure 5. Same as figure 3, but with $n = 3$.

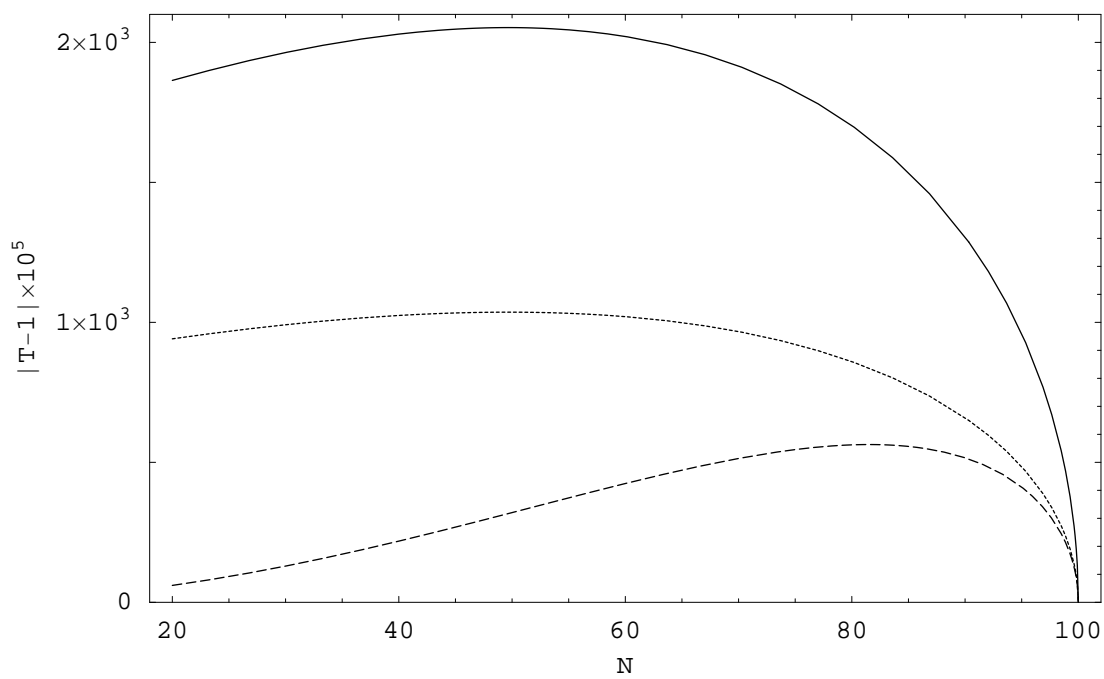


Figure 6. Same as figure 3, but with $n = 4$

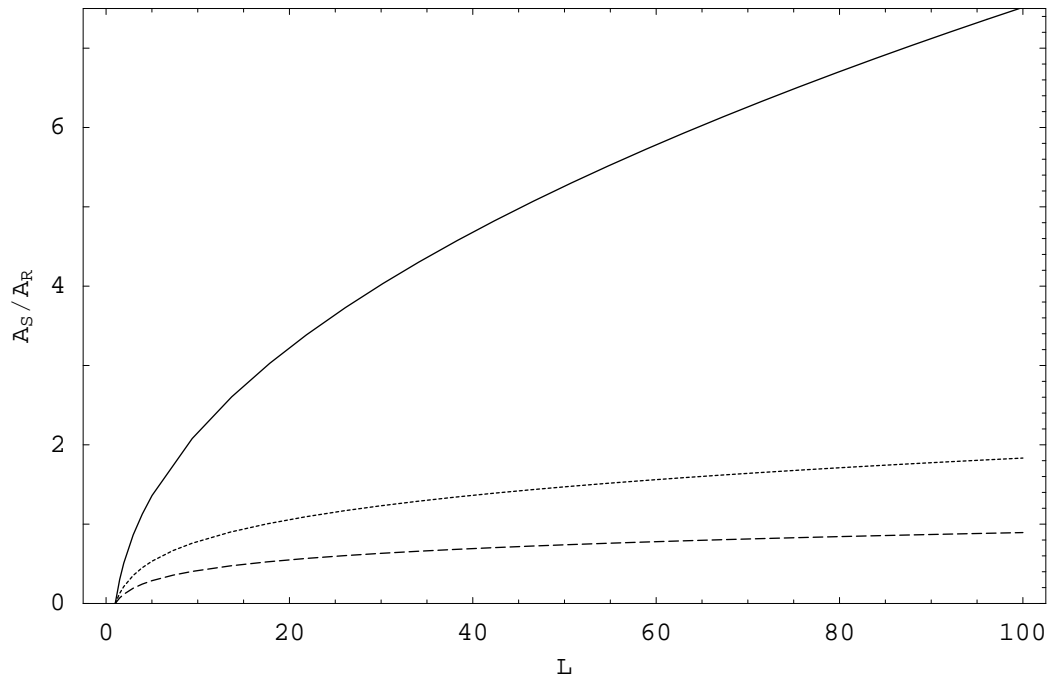


Figure 7. The ratio A_S/A_R at the time $N = 60$ as function of L for the models $n = 2, 3, 4$ (from top to bottom). Here we fixed $\lambda_1\lambda_2 = 10^{-24}$, and $N_* = 100$ is adopted.